

Thermal buckling analysis of functionally graded carbon nanotube-reinforced composite sandwich beams

Farzad Ebrahimi* and Navid Farazmandnia

Department of Mechanical Engineering, Faculty of Engineering, Imam Khomeini International University, Qazvin, Iran

(Received September 29, 2017, Revised January 19, 2018, Accepted February 20, 2018)

Abstract. Thermo-mechanical buckling of sandwich beams with a stiff core and face sheets made of functionally graded carbon nanotube-reinforced composite (FG-CNTRC) within the framework of Timoshenko beam theory is presented. The material properties of FG-CNTRC are supposed to vary continuously in the thickness direction and are estimated through the rule of mixture. Also the properties of these materials should be considered temperature dependent. The governing equations and boundary conditions are derived by using Hamilton's principle and solved using an efficient technique called the Differential Transform Method (DTM) to achieve the critical buckling of the sandwich beam in uniform thermal environment. A detailed parametric study is guided to investigate the effects of carbon nanotube volume fraction, slenderness ratio, core-to-face sheet thickness ratio, and clamped-clamped, simply-simply and clamped-simply end supports on the critical buckling behavior of sandwich beams with FG-CNTRC face sheets. Numerical results for comparison of sandwich beams with uniformly distributed carbon nanotube-reinforced composite (UD-CNTRC) face sheets with those with FG-CNTRC face sheets are also presented.

Keywords: buckling analysis; sandwich beam; FG-CNTRC; thermal environment

1. Introduction

The use of sandwich structures is growing so rapidly all over the world and has attracted increasing attention due to its super fantastic characteristics. The need of higher performances and lower weight of the structures makes sandwich construction one of the best choices applied in aircrafts, space vehicles and transportation systems. On the other hand, functionally graded materials (FGMs) are composite materials with inhomogeneous micromechanical structure in which the material properties of FGMs change smoothly between two surfaces. Also one of the advantages of this combination is novel structures that are capable to withstand large mechanical loadings under high temperature environments (Ebrahimi and Salari 2015a). Presenting novel properties, FGMs have also attracted intensive research interests, which were mainly focused on their static, buckling and vibration characteristics of FG structures (Ebrahimi and Salari 2015b, c, Ebrahimi and Barati 2016a-e, Ebrahimi *et al.* 2016, Ebrahimi and Dabbagh 2016, Ebrahimi and Hosseini 2016a, b). As a one of their applications we can mention the use of them in sandwich structures as face sheets. Because of this, many researches have been done on the vibration, buckling and post-buckling behaviors of sandwich structures with FGM face sheets, like these (Pradhan and Murmu 2009, Zenkour and Sobhy 2010).

Actually, material gradation will reduce maximum stresses and change the spatial location where such

maximums arise (Rahmani and Pedram 2014). This provides the opportunity of fitting material variation to attain desired stresses in a structure. The inspiration for using functionally graded materials (FGMs) is their advantages of superior stress relaxation and abilities of enduring high temperature gradients.

Carbon nanotubes (CNTs) have extraordinary mechanical properties. Ajayan *et al.* (1994) investigated polymer composites reinforced by aligned CNT arrays at first. Since then, many researchers inspected the material properties and functions of CNTRCs. Ashrafi and Hubert (2006) modeled the elastic properties of CNTRCs through a finite element analysis. Xu *et al.* (2006) examined the thermal behavior of SWCNT polymer-matrix composites. Han and Elliott (2007) used molecular dynamics (MD), to simulate the elastic properties of CNTRCs. These studies proved that adding a small amount of carbon nanotubes can significantly improve the electrical, mechanical, and thermal properties of polymeric composites. The results were as helpful for the prediction of the global response of CNTRCs as an actual structural constituents. Studies on CNTRCs have revealed that distributing CNTs in a uniform way as the reinforcements in matrix can lead to only intermediate improvement of the mechanical characteristics (Qian *et al.* 2000, Seidel and Lagoudas 2006). This is principally because of the weak interfacial bonding strength between the CNTs and matrix. Ke *et al.* (2010, 2013) examined the effect of FG-CNT volume fraction on the nonlinear free vibration and dynamic stability of composite beams. Shen (2011) performed a thermal post-buckling analysis for CNTRC cylindrical shells and learned that in general, the CNTRC shells with intermediate nanotube volume fraction do not support intermediate buckling

*Corresponding author, Associate Professor,
E-mail: febrahimi@eng.ikiu.ac.ir

temperature and initial thermal post-buckling strength.

The molecular bridging between CNT within the matrix is hopeful for enhancing nanocomposite's mechanical performance. One of the main problems for nanocomposites is the inadequate bonding between nonstructural reinforcement and the matrix. Ni-coating on CNT is an effective method to overcome the drawback of the inadequate strength. Duan *et al.* (2017) have interpreted such enhancing mechanism from the molecular-dynamics insights. They have discussed the pullout process of CNT and Ni-coated CNT against copper matrix while the effects of geometric parameters, including CNT length and diameter, are taken into consideration. Their results show that the interfacial strength is significantly improved after the Ni-coated CNT. In another work they investigated the damping capacity and mechanical strength of Ni-coated carbon nanotube reinforced copper-matrix nanocomposites and single-crystal copper using molecular dynamics (MD). It is found that the mechanical strength of copper can be significantly improved by the embedded Ni-coated CNT. Analysis of nano-structure's mechanical behaviors is one of recent interesting research topics. (Ebrahimi and Barati 2016f-n, 2017). Shen and Zhu (2012) inspected the sandwich plate with FG-CNTRC face sheets thermal post-buckling. They studied that the base stiffness, temperature change, CNT volume fraction, and the core-to-face sheet thickness ratio have considerable influences on compressive buckling and post-buckling behaviors of the sandwich plate, whereas their influence on the thermal post-buckling behavior is much less. Recently various beam/plate theories has been introduced. Wang and Shen (2011) studied the vibration of CNTRC plates in thermal environments. They mentioned that generally the CNTRC plates with symmetrical distribution of CNTs have lower natural frequencies, but lower linear to nonlinear frequency ratios than ones with unsymmetrical or uniform distribution of CNTs. Wu *et al.* (2015) investigated free vibration and buckling of sandwich beams which are reinforced with FG-CNTRCs face sheets based on a Timoshenko beam theory. However, by considering these materials as a thermo-dependent ones, the lack of inspecting the vibration and buckling of temperature dependent materials is felt.

In this paper the buckling of a sandwich beam with a stiff core and FG-CNTRC face sheets in thermal environments through the framework of Timoshenko beam theory, which is followed by the authors' previous work, is presented. The material characteristics of carbon nanotubes are supposed to change in the thickness direction in a functionally graded form. They are also can be calculated through a micromechanical model where the CNT efficiency parameter (η) is determined by matching the elastic modulus of CNTRCs calculated from the rule of mixture with those gained from the MDs simulations. The DT method established upon the Taylor series expansion is one of the effective mathematical techniques employed to solve differential equation problems (Yang and Xiang 2007). Malik and Dang (1998) firstly applied the DTM in vibration analysis of isotropic beams. In this paper, the DTM is used to solve linear vibration problems of sandwich beams. A parametric study is directed to explain the effects

of carbon nanotube volume fraction, slenderness ratio, core-to-face sheet thickness ratio, different thermal environment and boundary conditions on the free vibration properties of sandwich beams with FG-CNTRC face sheets. Numerical results for sandwich beams with uniformly carbon nanotube distribution reinforced composite (UD-CNTRC) are also demonstrated for validation and comparison.

2. Sandwich beam with CNTRC face sheets

Imagine a symmetric sandwich beam with the length of L , width b and total thickness h subjected to an axial load made by thermal expansion. As we can see in Fig. 1 the sandwich beam is made of two CNTRC face sheets which are both equal to h_f and have a stiff core layer of thickness h_c between. Two different types of support condition namely, simply supported-simply supported (S-S) and clamped-clamped (C-C) are considered individually. On the other hand, two distributions of CNTs, i.e., V functionally graded and uniform, are studied. The material properties can be determined through the rule of mixture

$$E_{11} = \eta V_{cn} E_{11}^{cn} + V_m E_m \quad (1a)$$

$$\frac{\eta_2}{E_{22}} = \frac{V_{cn}^*}{E_{22}^{cn}} + \frac{V_m}{E_{22}^m} \quad (1b)$$

$$\frac{\eta_3}{G_{12}} = \frac{V_{cn}^*}{G_{12}^{cn}} + \frac{V_m}{G_m} \quad (1c)$$

where E_{11}^{cn} , E_{22}^{cn} and G_{12}^{cn} are Young's moduli and shear modulus of CNTs, respectively. E_m and G_m are the properties for the matrix. η_i ($i = 1, 2, 3$) is CNT efficiency parameter accounting for the scale-dependent material properties and can be obtained by matching the elastic modulus of CNTRCs achieved from molecule dynamic simulation and those which are extracted from rule of mixture. V_m and V_{cn} are the volume fraction of matrix and the CNTs, respectively. The relation between them can be expressed as

$$V_{cn} + V_m = 1 \quad (2)$$

The material properties of functionally graded ceramic-metal composites, most commonly change along thickness

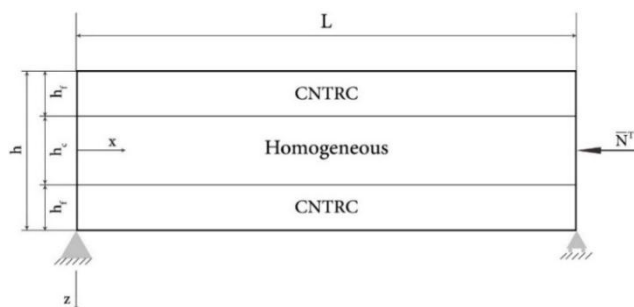


Fig. 1 A simple scheme of sandwich beam with CNTRC face sheets

direction in two ways; either a power law or an exponential distribution. However, in nanocomposites, the manufacturing method for such a graded distribution is so expensive and difficult. It is supposed that V_{cn} for the FG-CNTRC face sheets changes linearly across the thickness because aligning CNTs functionally graded in a polymer matrix leads to manufacture CNTRC in a better way, and only linear distribution can be obtained in engineering practice, so the distribution for the top face sheet can be expressed by

$$V_{cn} = \frac{-(2z + h_c)}{h_f} V_{cn}^* \quad (3a)$$

$$V_{cn} = \frac{(2z - h_c)}{h_f} V_{cn}^* \quad (3b)$$

and also for the bottom face sheet where V^* can be described as

$$V_{cn}^* = \frac{w_{cn}}{w_{cn} + \frac{\rho_{cn}}{\rho_m} - \frac{\rho_{cn}}{\rho_m} w_{cn}} \quad (4)$$

In this expression w_{cn} is the mass fraction of CNT, whereas ρ_m and ρ_{cn} are the densities of matrix and CNT, respectively. There is a simple relation for V_{cn}^* in UD-CNTRCs which can be given by $V_{cn} = V_{cn}^*$, so it's obvious that the mass fraction for UD-CNTRC and FG-CNTRC face sheets are equal.

The density and Poisson's ratio of the CNTRC face sheets can be described in v_{cn} order as

$$v = V_{cn} v_{cn} + V_m v_m \quad (5)$$

$$\rho = V_{cn} \rho_{cn} + V_m \rho_m \quad (6)$$

in which v_m and are Poisson's ratio of the matrix and CNT, respectively. Because functionally graded structures, such as sandwich beams in this case, are used mostly in high temperature environments, eventually magnificent changes in mechanical properties of the ingredient materials are to be expected, it is necessary to take into account this temperature-dependency for precise prediction of the mechanical reaction. Thus, Young's modulus and thermal expansion coefficient believed to be functions of temperature, as to be shown in Section 3.1, so that E and α are both temperature and position dependent. The behavior of FG materials can be predicted under high temperature more precisely with considering the temperature dependency on material properties. The nonlinear equation of thermo-elastic material properties in function of temperature $T(K)$ can be expressed as (Shen 2004)

$$P = P_0(P_{-1}T^{-1} + 1 + P_1T + P_2T^2 + P_3T^3) \quad (7)$$

where P_0, P_{-1}, P_1, P_2 and P_3 are the temperature dependent coefficients which can be seen in the table of materials properties (Table 1) for Ti-6Al-4V. For composite host,

Table 1 Temperature dependent properties of Young's modulus and thermal expansion coefficient for Ti-6Al-4V

Material	Properties	P_0	P_{-1}	P_1	P_2	P_3
Ti-6Al-4V	E (Pa)	122.56e+9	0	-4.586e-4	0	0
	α (K ⁻¹)	7.5788e-6	0	6.638e-4	-3.147e-6	0

Table 2 Temperature dependent properties of Young's modulus and thermal expansion coefficient for CNTs

Temperature (°K)	E_{11}^{cn} (TPa)	E_{22}^{cn} (TPa)	G_{12}^{cn} (TPa)	α^{cn} (K ⁻¹)
300	5.6466	7.0800	1.9445	3.4584
500	5.5308	6.9348	1.9643	4.5361
700	5.4744	6.8641	1.9644	4.6677

PMMA matrix have been chosen. Eventually there are different expressions to describe the temperature dependent properties of PMMA; $\alpha^m = 45(1+0.0005\Delta T) \times 10^{-6} /K$, $E^m = (3.52 - 0.0034T)$ GPa, in which $T = T_0 + \Delta T$ and $T_0 = 300$ K (Yang *et al.* 2015). However, there are not specific material properties expressions for CNTs. To predict the correct CNT properties which is dependent to temperature (Zhang and Shen 2006), we should estimate CNT efficiency parameters η_1 and η_2 by matching the Young's modulus E_{11} and E_{22} of CNTRCs obtained by the rule of mixture to those from the MD simulations given by Han and Elliott (2007). It should be noted that only E_{11} should be used in beam theories. The results are shown in Table 2.

3. Theoretical formulations

3.1 Governing equations

The displacement of an arbitrary point in the beam along the x and z directions, according to Timoshenko beam theory can be expressed by

$$\bar{U}(x, z, t) = U(x, t) + z\psi(x, t), \quad \bar{W}(x, z, t) = W(x, t), \quad (8)$$

where $U(x, t)$ and $W(x, t)$ are displacement elements of a point in the mid-plane, t is time and ψ is the rotation of the beam cross-section. The linear strain-displacement relationship can be described as

$$\varepsilon_{xx} = \frac{\partial U}{\partial x} + z \frac{\partial \psi}{\partial x}, \quad \gamma_{xz} = \frac{\partial W}{\partial x} + \psi. \quad (9)$$

The normal stress and shear stress are expressed as

$$\sigma_{xx} = Q_{11}(z) \left(\frac{\partial U}{\partial x} + z \frac{\partial \psi}{\partial x} \right), \quad \sigma_{xz} = Q_{55}(z) \left(\frac{\partial W}{\partial x} + \psi \right), \quad (10)$$

where

$$Q_{11}(z) = \frac{E(z)}{1-\nu^2}, \quad Q_{55}(z) = \frac{E(z)}{2(1+\nu)}. \quad (11)$$

The normal force, bending moment and transverse shear force resultants are presented as

$$N_x = \int_{-h/2}^{h/2} \sigma_{xx} dz = A_{11} \frac{\partial U}{\partial x} + B_{11} \frac{\partial \psi}{\partial x}, \quad (12a)$$

$$M_x = \int_{-h/2}^{h/2} \sigma_{xx} z dz = B_{11} \frac{\partial U}{\partial x} + D_{11} \frac{\partial \psi}{\partial x}, \quad (12b)$$

$$Q_x = \kappa \int_{-h/2}^{h/2} \sigma_{xz} dz = \kappa \left(A_{55} \frac{\partial W}{\partial x} + \psi \right), \quad (12c)$$

where the shear correction factor is expressed by $\kappa = 5/6$. The inertia related terms and stiffness components can be determined from

$$\{I_1, I_2, I_3\} = \int_{-h/2}^{h/2} \rho(z) \{1, z, z^2\} dz \quad (13a)$$

$$\{A_{11}, B_{11}, D_{11}\} = \int_{-h/2}^{h/2} Q_{11}(z) \{1, z, z^2\} dz, \quad (13b)$$

$$A_{55} = \int_{-h/2}^{h/2} Q_{55}(z) dz$$

Based on the Hamilton's principle, which states that the motion of an elastic structure during the time interval $t_1 < t < t_2$ is such that the time integral of the total dynamics potential is extremum (Tauchert 1974)

$$\int_0^t \delta(U - T + V) dt = 0 \quad (14)$$

Here U is strain energy, T is kinetic energy and V is work done by external forces. The virtual strain energy can be calculated as

$$\delta U = \int_v \sigma_{ij} \delta \varepsilon_{ij} dV = \int_v (\sigma_{xx} \delta \varepsilon_{xx} + \sigma_{xz} \delta \gamma_{xz}) dV \quad (15)$$

Substituting Eq. (9) into Eq. (15) gives

$$\delta U = \int_0^L (N \delta \frac{\partial U}{\partial x} + M \delta \frac{\partial \psi}{\partial x} + Q (\delta \frac{\partial W}{\partial x} + \delta \psi)) dx \quad (16)$$

The kinetic energy for Timoshenko beam theory can be inscribed as

$$T = \frac{1}{2} \int_0^L \int_A \rho(z, T) \left(\left(\frac{\partial U}{\partial t} \right)^2 + 2z \left(\frac{\partial U}{\partial t} \right) \left(\frac{\partial \psi}{\partial t} \right) + z^2 \left(\frac{\partial \psi}{\partial t} \right)^2 + \left(\frac{\partial W}{\partial t} \right)^2 \right) dA dx \quad (17)$$

Also the virtual kinetic energy can be expressed as

$$\delta T = \int_0^L \left[I_0 \left(\frac{\partial U}{\partial t} \frac{\partial \delta U}{\partial t} + \frac{\partial W}{\partial t} \frac{\partial \delta W}{\partial t} \right) + I_1 \left(\frac{\partial \psi}{\partial t} \frac{\partial \delta U}{\partial t} + \frac{\partial U}{\partial t} \frac{\partial \delta \psi}{\partial t} \right) + I_2 \frac{\partial \psi}{\partial t} \frac{\partial \delta \psi}{\partial t} \right] dx \quad (18)$$

The first variation of the work done corresponding to temperature change for a FG beam which has been in temperature environment for a long period of time, can be written in the form of

$$\delta V = \int_0^L \bar{N}^T \frac{\partial W}{\partial x} \frac{\partial \delta W}{\partial x} dx \quad (19)$$

also \bar{N}^T is thermal resultant and can be described as

$$\bar{N}^T = \int_{-h/2}^{h/2} E(z, T) \alpha(z, T) (T - T_0) dz \quad (20)$$

where T_0 is the reference temperature. Then by substituting Eqs. (16), (18) and (19) into Eq. (14) and setting the coefficients of δu , δw and $\delta \varphi$ to zero, the governing equations of motion of the beam can be defined as

$$\frac{\partial N_x}{\partial x} = I_1 \frac{\partial^2 U}{\partial t^2} + I_2 \frac{\partial^2 \psi}{\partial t^2}, \quad (21a)$$

$$\frac{\partial Q_x}{\partial x} - \bar{N}^T \frac{\partial^2 W}{\partial x^2} = I_1 \frac{\partial^2 W}{\partial t^2}, \quad (21b)$$

$$\frac{\partial M_x}{\partial x} - Q_x = I_2 \frac{\partial^2 U}{\partial t^2} + I_3 \frac{\partial^2 \psi}{\partial t^2}. \quad (21c)$$

where coefficient K_s is called the Timoshenko shear correction factor and the exact value of it depends on the material properties and cross section parameters of the beam. Here, K_s for rectangular beams has been assumed is equal to 5/6 approximately.

For simply supported-simply supported (S-S), clamped-clamped (C-C) and clamped-simply supported (C-S) sandwich beams with a movable end at $x = L$, the boundary conditions require

$$U = 0, \quad W = 0, \quad M_x = 0, \quad \text{at } x = 0, \quad (22a)$$

$$N_x = 0, \quad W = 0, \quad M_x = 0, \quad \text{at } x = L, \quad (22b)$$

for a S-S beam

$$U = 0, \quad W = 0, \quad \psi = 0, \quad \text{at } x = 0, \quad (23a)$$

$$N_x = 0, \quad W = 0, \quad \psi = 0, \quad \text{at } x = L, \quad (23b)$$

for a C-C beam and

$$U = 0, \quad W = 0, \quad \psi = 0, \quad \text{at } x = 0, \quad (24a)$$

$$N_x = 0, \quad W = 0, \quad M_x = 0, \quad \text{at } x = L, \quad (24b)$$

for a C-S beam.

3.2 Dimensionless governing equations

It is better first to clarify the following dimensionless quantities

$$\begin{aligned} \xi &= \frac{x}{L}, \quad (u, w) = \frac{(U, W)}{h}, \quad N^T = \frac{\bar{N}^T}{A_{110}}, \\ (\bar{I}_1, \bar{I}_2, \bar{I}_3) &= \left(\frac{I_1}{I_{10}}, \frac{I_2}{I_{10}h}, \frac{I_3}{I_{10}h^2} \right), \quad \varphi = \psi, \\ \lambda &= \frac{L}{h}, \quad \tau = \frac{t}{L} \sqrt{\frac{A_{110}}{I_{10}}}, \\ (a_{11}, a_{55}, b_{11}, d_{11}) &= \left(\frac{A_{11}}{A_{110}}, \kappa \frac{A_{55}}{A_{110}}, \frac{B_{11}}{A_{110}h}, \frac{D_{11}}{A_{110}h^2} \right), \end{aligned} \quad (25)$$

where I_{10} and A_{110} are the values of I_1 and A_{11} of a homogeneous beam made from pure core material. With respect to Eqs. (25), and substituting Eqs. (12) into Eqs. (21), the final equations can then be explained in dimensionless form as

$$a_{11} \frac{\partial^2 u}{\partial \zeta^2} + b_{11} \frac{\partial^2 \varphi}{\partial \zeta^2} = \bar{I}_1 \frac{\partial^2 u}{\partial \tau^2} + \bar{I}_2 \frac{\partial^2 \varphi}{\partial \tau^2}, \quad (26a)$$

$$a_{55} \left(\frac{\partial^2 w}{\partial \zeta^2} + \lambda \frac{\partial \varphi}{\partial \zeta} \right) - N^T \frac{\partial^2 w}{\partial \zeta^2} = \bar{I}_1 \frac{\partial^2 w}{\partial \tau^2}, \quad (26b)$$

$$b_{11} \frac{\partial^2 u}{\partial \zeta^2} + d_{11} \frac{\partial^2 \varphi}{\partial \zeta^2} - a_{55} \lambda \left(\frac{\partial w}{\partial \zeta} + \lambda \varphi \right) = \bar{I}_2 \frac{\partial^2 u}{\partial \tau^2} + \bar{I}_3 \frac{\partial^2 \varphi}{\partial \tau^2}, \quad (26c)$$

and the transformed boundary conditions turn into

$$u = 0, \quad w = 0, \quad \varphi = 0, \quad \text{at } \zeta = 0, \quad (27a)$$

$$a_{11} \frac{\partial u}{\partial \zeta} + b_{11} \frac{\partial \varphi}{\partial \zeta}, \quad w = 0, \quad \varphi = 0, \quad \text{at } \zeta = L, \quad (27b)$$

for a S-S sandwich beam

$$u = 0, \quad w = 0, \quad b_{11} \frac{\partial u}{\partial \zeta} + d_{11} \frac{\partial \varphi}{\partial \zeta} = 0, \quad \text{at } \zeta = 0, \quad (28a)$$

$$a_{11} \frac{\partial u}{\partial \zeta} + b_{11} \frac{\partial \varphi}{\partial \zeta}, \quad w = 0, \quad b_{11} \frac{\partial u}{\partial \zeta} + d_{11} \frac{\partial \varphi}{\partial \zeta} = 0, \quad (28b)$$

at $\zeta = L$,

for a C-C sandwich beam and

$$u = 0, \quad w = 0, \quad \varphi = 0, \quad \text{at } \zeta = 0, \quad (29a)$$

$$a_{11} \frac{\partial u}{\partial \zeta} + b_{11} \frac{\partial \varphi}{\partial \zeta}, \quad w = 0, \quad b_{11} \frac{\partial u}{\partial \zeta} + d_{11} \frac{\partial \varphi}{\partial \zeta} = 0, \quad (29b)$$

at $\zeta = L$,

for a C-S sandwich beam.

4. Uniform temperature rise (UTR)

The sandwich beam initial temperature is assumed to be ($T_0 = 300$ K), which is a stress free state, uniformly changed

to final temperature with ΔT . The temperature rise is given by

$$\Delta T = T - T_0 \quad (30)$$

5. Solution procedure

5.1 Application of differential transform method (DTM) to buckling problem

In this section, DTM is performed to solving equations of motions, which is a semi-analytic transformation technique based on Taylor series expansion equations and is a useful tool to obtain analytical solutions of these differential equations. Certain transformations rules are applied to governing equations and the boundary conditions of the system in order to transform them into a set of algebraic equations in terms of the differential transforms of the original functions. This method constructs an analytical solution in the form of polynomials. It is different from the high-order Taylor series method, which requires symbolic computation of the necessary derivative of the data functions and is expensive for large orders. The Taylor series method is computationally expansive for large orders. DTM is an iterative procedure for obtaining analytic Taylor series solutions of differential equations; in fact, this method tries to find coefficients of series expansions of unknown function with using the initial data on the problem.

Differential transformation of the nth derivative function $y(x)$ and differential inverse transformation of $Y(k)$ are respectively defined as follow (Hassan 2002)

$$Y(k) = \frac{1}{k!} \left[\frac{d^k}{dx^k} y(x) \right]_{x=0} \quad (31)$$

$$y(x) = \sum_{k=0}^{\infty} X^k Y(k) \quad (32)$$

in which $y(x)$ is the original function and $Y(k)$ is the transformed function. Consequently, from Eqs. (31) and (32) can obtain

$$Y(k) = \sum_{k=0}^{\infty} \frac{x^k}{k!} \left[\frac{d^k}{dx^k} y(x) \right]_{x=0} \quad (33)$$

In this calculations N is determined by the convergence of the eigenvalues and $y(x)$ is small enough to be neglected. From definitions of DTM in Eqs. (31)-(33), the fundamental theorems of differential transforms method can be performed that are listed in Tables 3 and 4 present the differential transformation of conventional boundary conditions. Assuming a sinusoidal variation of $w(x, t)$ and $\theta(x, t)$, which the functions are approximated as

$$w(x, t) = \bar{w} e^{i\alpha x} \quad \theta(x, t) = \bar{\theta} e^{i\alpha x} \quad (34)$$

By reducing u and substituting Eqs. (34) into Eqs. (26) equations of motions have been turned to

Table 3 Some of the transformation rules of the one-dimensional DTM (Ju 2004)

Original function	Transformed function
$f(x) = g(x) \pm h(x)$	$F(K) = G(K) \pm H(K)$
$f(x) = \lambda g(x)$	$F(K) = \lambda G(K)$
$f(x) = g(x)h(x)$	$F(K) = \sum_{l=0}^K G(K-l)H(l)$
$f(x) = \frac{d^n g(x)}{dx^n}$	$F(K) = \frac{(k+n)!}{k!} G(K+n)$
$f(x) = x^n$	$F(K) = \delta(K-n) = \begin{cases} 1 & k=n \\ 0 & k \neq n \end{cases}$

$$a_{55} \left(\frac{\partial^2 w}{\partial \zeta^2} + \lambda \frac{\partial \varphi}{\partial \zeta} \right) - N_T \frac{\partial^2 w}{\partial \zeta^2} = -I_1 \omega^2 w(\zeta) \tag{35}$$

$$-\frac{b_{11}^2}{a_{11}} \frac{\partial^2 \varphi}{\partial \zeta^2} + d_{11} \frac{\partial^2 \varphi}{\partial \zeta^2} - a_{55} \lambda \left(\frac{\partial w}{\partial \zeta} + \lambda \varphi \right) = \bar{I}_2 \omega^2 \frac{b_{11}}{a_{11}} \varphi - \bar{I}_3 \omega^2 \varphi \tag{36}$$

According to the basic transformation operations in Table 3, the transformed form of the governing Eqs. (35) and (36) around $x_0 = 0$ may be obtained as

$$a_{55}(k+1)(k+2)w(k+2) + a_{55}\lambda(k+1)\varphi(k+1) - N_T(k+1)(k+2)w(k+2) = -I_1 \omega^2 w(k) \tag{37}$$

$$\left(d_{11} - \frac{b_{11}^2}{a_{11}} \right) (k+1)(k+2)\varphi(k+2) - a_{55}\lambda[(k+1)w(k+1) + \lambda\varphi] = -\omega^2 \left(\bar{I}_3 \varphi - \bar{I}_2 \frac{b_{11}}{a_{11}} \varphi \right) \tag{38}$$

Transformed functions of $W(x)$, $\psi(x)$ are $w(k)$, $\varphi(k)$, by using the theorems introduced in Table 4, transformed

various boundary conditions can be expressed as follow:

- Simply Supported-Simply supported:

$$w[0] = 0, \varphi[1] = 0$$

$$\sum_{k=0}^{\infty} w[k] = 0, \sum_{k=0}^{\infty} k \varphi[k] = 0 \tag{39a}$$

- Clamped-Simply supported:

$$w[0] = 0, \varphi[0] = 0$$

$$\sum_{k=0}^{\infty} w[k] = 0, \sum_{k=0}^{\infty} k \varphi[k] = 0 \tag{39b}$$

- Clamped-Clamped

$$w[0] = 0, \varphi[0] = 0$$

$$\sum_{k=0}^{\infty} w[k] = 0, \sum_{k=0}^{\infty} \varphi[k] = 0 \tag{39c}$$

by using Eqs. (37) and (38) together with the transformed boundary conditions one arrives at the following eigenvalue problem

$$\begin{bmatrix} M_{11}^{(n)}(\omega) & M_{12}^{(n)}(\omega) \\ M_{21}^{(n)}(\omega) & M_{22}^{(n)}(\omega) \end{bmatrix} [C] = 0 \tag{40}$$

where $[C]$ corresponds to the missing boundary conditions at $x = 0$ and M_{ij} are polynomials in terms of (ω) corresponding to the n th term. For the non-trivial solutions of Eq. (40), it is necessary that the determinant of the coefficient matrix set equal to zero

$$\begin{bmatrix} M_{11}^{(n)}(\omega) & M_{12}^{(n)}(\omega) \\ M_{21}^{(n)}(\omega) & M_{22}^{(n)}(\omega) \end{bmatrix} = 0 \tag{41}$$

The i th estimated eigenvalue may be obtained by for the n th iteration, by solving Eq. (41). The total number of iterations is related to the accuracy of calculations which

Table 4 Transformed boundary conditions (B.C.) based on DTM (Ju 2004)

$x = 0$		$x = L$	
Original B.C.	Transformed B.C.	Original B.C.	Transformed B.C.
$f(0) = 0$	$F[0] = 0$	$f(L) = 0$	$\sum_{k=0}^{\infty} F[k] = 0$
$\frac{df(0)}{dx} = 0$	$F[1] = 0$	$\frac{df(L)}{dx} = 0$	$\sum_{k=0}^{\infty} k F[k] = 0$
$\frac{d^2 f(0)}{dx^2} = 0$	$F[2] = 0$	$\frac{d^2 f(L)}{dx^2} = 0$	$\sum_{k=0}^{\infty} k(k-1)F[k] = 0$
$\frac{d^3 f(0)}{dx^3} = 0$	$F[3] = 0$	$\frac{d^3 f(L)}{dx^3} = 0$	$\sum_{k=0}^{\infty} k(k-1)(k-2)F[k] = 0$

can be determined by following equations

$$|\omega_i^{(n)} - \omega_i^{(n-1)}| < \varepsilon \tag{42}$$

In this study $\varepsilon = 0.0001$ in procedure of finding eigenvalues results in four-digit precision is estimated eigenvalues. Further the computer package Mathematica has been developed according to the DTM rules as stated

Table 5 Convergence study for the critical buckling load for C-C sandwich beams with FG-CNTRC face sheets ($V_{cn}^* = 0.12, L/h = 10, h_c/h_f = 8$)

n	N_{cr}
9	-
10	-
11	0.02975
12	0.02243
13	0.02425
14	0.02371
15	0.02723
16	0.02690
17	0.02583
18	0.02583
19	0.02591
20	0.02591
21	0.02591
22	0.02591
23	0.02591

before to find eigenvalues. As mentioned before, DT method implies an iterative procedure to obtain the high-order Taylor series solution of differential equations. The Taylor series method requires a long computational time for large orders, whereas one advantage of employing DTM in solving differential equations is a fast convergence rate and small calculation error.

6. Results and discussion

6.1 Comparison studies

Before starting to study the buckling analysis of sandwich beams with CNTRC face sheets, a comparison is made between our results and those from the open literature are made to validate the present formulation. Table 5 shows the number of repetition for convergence of the critical buckling using DTM method. It is found that in DTM method after a certain number of iterations eigenvalues converged to a value with good precision, so the number of iterations is important in DTM method convergence. According to Table 5 the critical buckling converged after 15 iterations with 4-digit precision. Table 6 compares numerical dimensionless critical buckling of simply-simply supported ends FGM sandwich beams with the semi analytical results (Wu *et al.* 2015) from which the material properties used in this comparison can be found. As it can be seen, our results match very well with the results of reference paper. The dimensionless critical buckling for the C-C FG-CNTRC beam are tabulated in Table 7 also. The parameters used in this example are the same as those in Ref. (Wu *et al.* 2015). A good agreement is obtained, again.

Table 6 Comparison of dimensionless critical buckling of S-S sandwich beams with FG-CNTRC face sheets ($h_c/h_f = 8$)

L/h		$V_{cn}^* = 0.12$		$V_{cn}^* = 0.17$		$V_{cn}^* = 0.28$	
		Present	(Wu <i>et al.</i> 2015)	Present	(Wu <i>et al.</i> 2015)	Present	(Wu <i>et al.</i> 2015)
10	FG	0.0071	0.0072	0.0086	0.0085	0.0115	0.0111
	UD	0.0069	0.0070	0.0083	0.0082	0.0110	0.0107
20	FG	0.0018	0.0018	0.0022	0.0022	0.0029	0.0029
	UD	0.0018	0.0018	0.0021	0.0021	0.0028	0.0028
30	FG	0.0008	0.0008	0.0010	0.0010	0.0013	0.0013
	UD	0.0008	0.0008	0.0009	0.0009	0.0012	0.0012

Table 7 Comparison of dimensionless critical buckling of C-C sandwich beams with FG-CNTRC face sheets ($h_c/h_f = 8$)

L/h		$V_{cn}^* = 0.12$		$V_{cn}^* = 0.17$		$V_{cn}^* = 0.28$	
		Present	(Wu <i>et al.</i> 2015)	Present	(Wu <i>et al.</i> 2015)	Present	(Wu <i>et al.</i> 2015)
10	FG	0.0259	0.0261	0.0309	0.0305	0.0408	0.0387
	UD	0.0252	0.0254	0.0305	0.0296	0.0400	0.0373
20	FG	0.0071	0.0072	0.0088	0.0085	0.0113	0.0111
	UD	0.0069	0.0070	0.0083	0.0082	0.0110	0.0107
30	FG	0.0032	0.0032	0.0039	0.0039	0.0051	0.0051
	UD	0.0031	0.0037	0.0038	0.0037	0.0050	0.0049

Table 8 Effect of nanotube volume fraction and slenderness ratio on dimensionless critical buckling of sandwich beams with FG-CNTRC face sheets ($h_c/h_f = 8$)

L/h	B.S.		$\Delta T = 0$			$\Delta T = 200$			$\Delta T = 400$		
			V_{cn}^*			V_{cn}^*			V_{cn}^*		
			0.12	0.17	0.28	0.12	0.17	0.28	0.12	0.17	0.28
10	S-S	FG	0.0071	0.0086	0.0115	0.0066	0.0082	0.0109	0.0062	0.0076	0.0104
	S-S	UD	0.0069	0.0083	0.0110	0.0064	0.0079	0.0105	0.0060	0.0073	0.0099
20	S-S	FG	0.0018	0.0022	0.0029	0.0017	0.0020	0.0028	0.0016	0.0019	0.0026
	S-S	UD	0.0018	0.0021	0.0028	0.0017	0.0018	0.0027	0.0015	0.0018	0.0025
30	S-S	FG	0.0018	0.0010	0.0013	0.0007	0.0009	0.0012	0.0007	0.0008	0.0011
	S-S	UD	0.0018	0.0009	0.0012	0.0007	0.0008	0.0011	0.0007	0.0008	0.0011
10	C-C	FG	0.0259	0.0309	0.0408	0.0240	0.0290	0.0376	0.0227	0.0276	0.0373
	C-C	UD	0.0252	0.0305	0.0400	0.0234	0.0281	0.0367	0.0226	0.0266	0.0365
20	C-C	FG	0.0071	0.0088	0.0113	0.0065	0.0079	0.0105	0.0062	0.0076	0.0103
	C-C	UD	0.0069	0.0083	0.0110	0.0063	0.0077	0.0103	0.0061	0.0072	0.0101
30	C-C	FG	0.0032	0.0039	0.0051	0.0029	0.0036	0.0046	0.0028	0.0034	0.0047
	C-C	UD	0.0031	0.0038	0.0050	0.0028	0.0034	0.0045	0.0027	0.0033	0.0046

Table 9 Effect of nanotube volume fraction and h_c/h_f on dimensionless critical buckling of sandwich beams with FG-CNTRC face sheets ($L/h = 20$)

L/h	B.S.		$\Delta T = 0$			$\Delta T = 200$			$\Delta T = 400$		
			V_{cn}^*			V_{cn}^*			V_{cn}^*		
			0.12	0.17	0.28	0.12	0.17	0.28	0.12	0.17	0.28
8	S-S	FG	0.0018	0.0022	0.0029	0.0017	0.0020	0.0028	0.0016	0.0019	0.0026
	S-S	UD	0.0018	0.0021	0.0028	0.0016	0.0018	0.0027	0.0015	0.0018	0.0025
6	S-S	FG	0.0018	0.0023	0.0032	0.0017	0.0021	0.0030	0.0016	0.0020	0.0029
	S-S	UD	0.0017	0.0022	0.0030	0.0016	0.0020	0.0028	0.0015	0.0019	0.0027
4	S-S	FG	0.0019	0.0024	0.0036	0.0017	0.0023	0.0034	0.0016	0.0022	0.0033
	S-S	UD	0.0017	0.0022	0.0033	0.0016	0.0021	0.0031	0.0015	0.0020	0.0029
8	C-C	FG	0.0071	0.0088	0.0113	0.0065	0.0079	0.0105	0.0062	0.0076	0.0103
	C-C	UD	0.0069	0.0083	0.0110	0.0063	0.0077	0.0103	0.0061	0.0072	0.0101
6	C-C	FG	0.0071	0.0088	0.0122	0.0066	0.0083	0.0117	0.0063	0.0080	0.0114
	C-C	UD	0.0067	0.0083	0.0115	0.0063	0.0079	0.0110	0.0060	0.0076	0.0107
4	C-C	FG	0.0071	0.0093	0.0136	0.0068	0.0089	0.0131	0.0065	0.0087	0.0129
	C-C	UD	0.0066	0.0086	0.0124	0.0064	0.0082	0.0119	0.0060	0.0079	0.0117

6.2 Static buckling

In this study, poly (methyl methacrylate), i.e., PMMA with $E_m = 2.5$ GPa, $\rho_m = 1190$ kg/m³ and $\nu_m = 0.3$, are chosen to be the matrix material for CNTRCs. The armchair (10, 10) SWCNTs, with material properties of $E_{11}^{cn} = 5.6466$ TPa, $E_{22}^{cn} = 7.08$ TPa, $G_{12}^{cn} = 1.9445$ TPa, $\rho_{cn} = 1400$ kg/m³ and $\nu_m = 0.175$ at room temperature, (Shen and Zhang 2010) are selected as the reinforcement for CNTRCs. The CNT efficiency parameter η_j is obtained by matching the Young's modulus E_{11} and E_{22} and shear modulus G_{12} of CNTRCs determined from the rule of mixture against those from the MD simulations given by Han and Elliott (2007). It was presented by Shen and Zhang (2010) as, $\eta_1 = 0.137$,

$\eta_2 = 1.022$, $\eta_3 = 0.715$ are used for the case of $V_{cn}^* = 0.12$, $\eta_1 = 0.142$, $\eta_2 = 1.626$, $\eta_3 = 1.138$ for $V_{cn}^* = 0.17$; and $\eta_1 = 0.141$, $\eta_2 = 1.585$, $\eta_3 = 1.109$ for $V_{cn}^* = 0.28$. We choose Titanium alloy (Ti-6Al-4V) for core, because when the core material has a lower strength, they cannot be predicted through the sandwich beam theory. Titanium alloy has $E_c = 113.8$ GPa, $\rho_c = 4430$ kg/m³ and $\nu_c = 0.342$, is selected as the core material for the sandwich beam. The thickness of the sandwich beam is chosen 10 mm totally, and kept steady in all numerical situations. However, the thickness of core layer and face sheets change arbitrarily as the core-to-face sheet thickness ratio is chosen $h_c/h_f = 8, 6, 4$. The critical buckling with respect to effect of initial thermal environment are given in Tables 8 and 9.

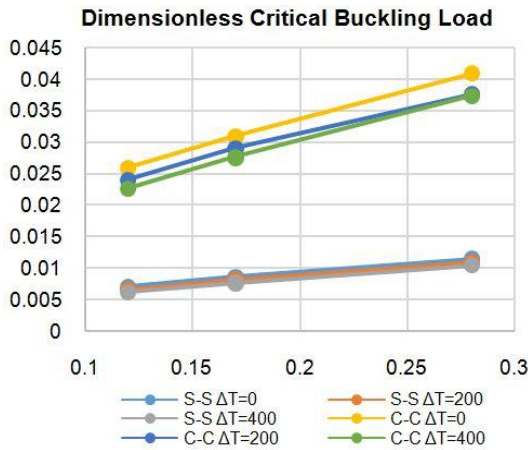


Fig. 2 Dimensionless critical buckling load of C-C and S-S sandwich beams with CNTRC face sheets with different slenderness ratio L/h , nanotube volume fraction and temperature difference

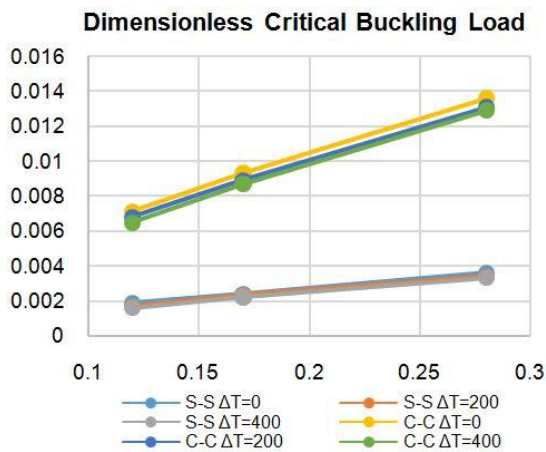


Fig. 3 Dimensionless critical buckling load of C-C and S-S sandwich beams with CNTRC face sheets with different core-to-face sheet thickness ratio h_c/h_f , nanotube volume fraction and temperature difference

Table 8 and Fig. 2, present the dimensionless critical buckling of C-C and S-S sandwich beams with CNTRC face sheets with different slenderness ratio L/h , nanotube volume fraction and temperature difference. The core-to-face sheet thickness ratio is kept unchanged at $h_c/h_f = 8$. It is observed that the critical buckling of the sandwich beam decreases with an increase in the slenderness ratio and temperature. The C-C sandwich beam has a higher critical buckling than the same S-S one. Furthermore, it is observed that the critical buckling of the sandwich beam with UD-CNTRC face sheets is also lower than that of the beam with FG-CNTRC face sheets. This is because the sandwich beam with UD-CNTRC face sheets has a lower stiffness than the beam with FG-CNTRC face sheets.

Table 9 and Fig. 3, present the dimensionless critical buckling of C-C and S-S sandwich beams with CNTRC face sheets with different core-to-face sheet thickness ratio h_c/h_f , nanotube volume fraction and temperature difference.

The slenderness ratio is kept unchanged at $L/h = 20$. It is observed that the critical buckling of the sandwich beam increases with a decrease in core-to-face sheet thickness ratio but decreases when temperature increases. The C-C sandwich beam has a higher critical buckling than the same S-S one. Furthermore, it is observed that the critical buckling of the sandwich beam with UD-CNTRC face sheets is also lower than that of the beam with FG-CNTRC face sheets. This is because the sandwich beam with UD-CNTRC face sheets has a lower stiffness than the beam with FG-CNTRC face sheets.

7. Conclusions

Thermo-mechanical buckling characteristics of sandwich beams with CNTRC face sheets have been examined based on the Timoshenko beam theory and semi analytical DT method. The effects of CNT volume fraction, core-to-face sheet thickness ratio, slenderness ratio, and end supporting conditions on the free vibration behaviors of stiff-cored sandwich beams with CNTRC face sheets with respect to uniform temperature change revealed through a parametric study. Numerical results show that CNT volume fraction, end supporting conditions, and slenderness ratio have a significant influence on the natural frequencies, whereas the effects of temperature change and core-to-face sheet thickness ratio is much less pronounced. The static buckling of the sandwich beam decrease with an increase in temperature change, core-to-face and slenderness ratio, but they increase with an increase in CNT volume fraction. The numerical results also point out that the sandwich beam with UD-CNTRC face sheets has lower buckling performances than FG-CNTRC the beam with face sheets.

References

Ajayan, P.M., Stephan, O., Colliex, C. and Trauth, D. (1994), "Aligned carbon nanotube arrays formed by cutting a polymer resin—nanotube composite", *Science*, **265**(5176), 1212-1214.

Ashrafi, B. and Hubert, P. (2006), "Modeling the elastic properties of carbon nanotube array/polymer composites", *Compos. Sci. Technol.*, **66**(3), 387-396.

Duan, K., Li, L., Hu, Y. and Wang, X. (2017), "Enhanced interfacial strength of carbon nanotube/copper nanocomposites via Ni-coating: Molecular-dynamics insights", *Physica E: Low-Dimens. Syst. Nanostruct.*, **88**, 259-264.

Ebrahimi, F. and Barati, M.R. (2016a), "Temperature distribution effects on buckling behavior of smart heterogeneous nanosize plates based on nonlocal four-variable refined plate theory", *Int. J. Smart Nano Mater.*, **7**(3), 119-143.

Ebrahimi, F. and Barati, M.R. (2016b), "Vibration analysis of smart piezoelectrically actuated nanobeams subjected to magneto-electrical field in thermal environment", *J. Vib. Control*, 1077546316646239.

Ebrahimi, F. and Barati, M.R. (2016c), "Size-dependent thermal stability analysis of graded piezomagnetic nanoplates on elastic medium subjected to various thermal environments", *Appl. Phys. A*, **122**(10), 910.

Ebrahimi, F. and Barati, M.R. (2016d), "Static stability analysis of smart magneto-electro-elastic heterogeneous nanoplates embedded in an elastic medium based on a four-variable refined

- plate theory”, *Smart Mater. Struct.*, **25**(10), 105014.
- Ebrahimi, F. and Barati, M.R. (2016e), “Buckling analysis of piezoelectrically actuated smart nanoscale plates subjected to magnetic field”, *J. Intel. Mater. Syst. Struct.*, **28**(11), 1472-1490.
- Ebrahimi, F. and Barati, M.R. (2016f), “A nonlocal higher-order shear deformation beam theory for vibration analysis of size-dependent functionally graded nanobeams”, *Arab. J. Sci. Eng.*, **41**(5), 1679-1690.
- Ebrahimi, F. and Barati, M.R. (2016g), “Vibration analysis of nonlocal beams made of functionally graded material in thermal environment”, *Eur. Phys. J. Plus*, **131**(8), 279.
- Ebrahimi, F. and Barati, M.R. (2016h), “Dynamic modeling of a thermo-piezo-electrically actuated nanosize beam subjected to a magnetic field”, *Appl. Phys. A*, **122**(4), 1-18.
- Ebrahimi, F. and Barati, M.R. (2016i), “A unified formulation for dynamic analysis of nonlocal heterogeneous nanobeams in hygro-thermal environment”, *Appl. Phys. A*, **122**(9), 792.
- Ebrahimi, F. and Barati, M.R. (2016j), “A nonlocal higher-order refined magneto-electro-viscoelastic beam model for dynamic analysis of smart nanostructures”, *Int. J. Eng. Sci.*, **107**, 183-196.
- Ebrahimi, F. and Barati, M.R. (2016k), “Hygrothermal effects on vibration characteristics of viscoelastic FG nanobeams based on nonlocal strain gradient theory”, *Compos. Struct.*, **159**, 433-444.
- Ebrahimi, F. and Barati, M.R. (2016l), “Buckling analysis of nonlocal third-order shear deformable functionally graded piezoelectric nanobeams embedded in elastic medium”, *J. Brazil. Soc. Mech. Sci. Eng.*, **39**(3), 937-952.
- Ebrahimi, F. and Barati, M.R. (2016m), “Magnetic field effects on buckling behavior of smart size-dependent graded nanoscale beams”, *Eur. Phys. J. Plus*, **131**(7), 1-14.
- Ebrahimi, F. and Barati, M.R. (2016n), “Buckling analysis of smart size-dependent higher order magneto-electro-thermo-elastic functionally graded nanosize beams”, *J. Mech.*, **33**(1), 23-33.
- Ebrahimi, F. and Barati, M.R. (2017), “A nonlocal strain gradient refined beam model for buckling analysis of size-dependent shear-deformable curved FG nanobeams”, *Compos. Struct.*, **159**, 174-182.
- Ebrahimi, F. and Dabbagh, A. (2016), “On flexural wave propagation responses of smart FG magneto-electro-elastic nanoplates via nonlocal strain gradient theory”, *Compos. Struct.*, **162**, 281-293.
- Ebrahimi, F. and Hosseini, S.H.S. (2016a), “Thermal effects on nonlinear vibration behavior of viscoelastic nanosize plates”, *J. Therm. Stress.*, **39**(5), 606-625.
- Ebrahimi, F. and Hosseini, S.H.S. (2016b), “Double nanoplate-based NEMS under hydrostatic and electrostatic actuations”, *Eur. Phys. J. Plus*, **131**(5), 1-19.
- Ebrahimi, F. and Salari, E. (2015a), “Thermal buckling and free vibration analysis of size dependent Timoshenko FG nanobeams in thermal environments”, *Compos. Struct.*, **128**, 363-380.
- Ebrahimi, F. and Salari, E. (2015b), “Size-dependent free flexural vibrational behavior of functionally graded nanobeams using semi-analytical differential transform method”, *Compos. Part B: Eng.*, **79**, 156-169.
- Ebrahimi, F. and Salari, E. (2015c), “Nonlocal thermo-mechanical vibration analysis of functionally graded nanobeams in thermal environment”, *Acta Astronautica*, **113**, 29-50.
- Ebrahimi, F., Ghadiri, M., Salari, E., Hoseini, S.A.H. and Shaghghi, G.R. (2015a), “Application of the differential transformation method for nonlocal vibration analysis of functionally graded nanobeams”, *J. Mech. Sci. Technol.*, **29**(3), 1207-1215.
- Ebrahimi, F., Salari, E. and Hosseini, S.A.H. (2015b), “Thermomechanical vibration behavior of FG nanobeams subjected to linear and nonlinear temperature distributions”, *J. Therm. Stress.*, **38**(12), 1360-1386.
- Ebrahimi, F., Barati, M.R. and Dabbagh, A. (2016), “A nonlocal strain gradient theory for wave propagation analysis in temperature-dependent inhomogeneous nanoplates”, *Int. J. Eng. Sci.*, **107**, 169-182.
- Han, Y. and Elliott, J. (2007), “Molecular dynamics simulations of the elastic properties of polymer/carbon nanotube composites”, *Computat. Mater. Sci.*, **39**(2), 315-323.
- Hassan, I.A.-H. (2002), “On solving some eigenvalue problems by using a differential transformation”, *Appl. Math. Computat.*, **127**(1), 1-22.
- Ju, S.-P. (2004), “Application of differential transformation to transient advective-dispersive transport equation”, *Appl. Math. Computat.*, **155**(1), 25-38.
- Ke, L.L., Yang, J. and Kitipornchai, S. (2010), “Nonlinear free vibration of functionally graded carbon nanotube-reinforced composite beams”, *Compos. Struct.*, **92**(3), 676-683.
- Ke, L.L., Yang, J. and Kitipornchai, S. (2013), “Dynamic stability of functionally graded carbon nanotube-reinforced composite beams”, *Mech. Adv. Mater. Struct.*, **20**(1), 28-37.
- Malik, M. and Dang, H.H. (1998), “Vibration analysis of continuous systems by differential transformation”, *Appl. Math. Computat.*, **96**(1), 17-26.
- Pradhan, S. and Murmu, T. (2009), “Thermo-mechanical vibration of FGM sandwich beam under variable elastic foundations using differential quadrature method”, *J. Sound Vib.*, **321**(1), 342-362.
- Qian, D., Dickey, E.C., Andrews, R. and Rantell, T. (2000), “Load transfer and deformation mechanisms in carbon nanotube-polystyrene composites”, *Appl. Phys. Lett.*, **76**(20), 2868-2870.
- Rahmani, O. and Pedram, O. (2014), “Analysis and modeling the size effect on vibration of functionally graded nanobeams based on nonlocal Timoshenko beam theory”, *Int. J. Eng. Sci.*, **77**, 55-70.
- Seidel, G.D. and Lagoudas, D.C. (2006), “Micromechanical analysis of the effective elastic properties of carbon nanotube reinforced composites”, *Mech. Mater.*, **38**(8), 884-907.
- Shen, H.-S. (2004), “Thermal postbuckling behavior of functionally graded cylindrical shells with temperature-dependent properties”, *Int. J. Solids Struct.*, **41**(7), 1961-1974.
- Shen, H.-S. (2011), “Postbuckling of nanotube-reinforced composite cylindrical shells in thermal environments, Part II: Pressure-loaded shells”, *Compos. Struct.*, **93**(10), 2496-2503.
- Shen, H.-S. and Zhu, Z. (2012), “Postbuckling of sandwich plates with nanotube-reinforced composite face sheets resting on elastic foundations”, *Eur. J. Mech.-A/Solids*, **35**, 10-21.
- Tauchert, T.R. (1974), *Energy Principles in Structural Mechanics*, McGraw-Hill Companies.
- Wang, Z.-X. and Shen, H.-S. (2011), “Nonlinear vibration of nanotube-reinforced composite plates in thermal environments”, *Computat. Mater. Sci.*, **50**(8), 2319-2330.
- Wu, H., Kitipornchai, S. and Yang, J. (2015), “Free vibration and buckling analysis of sandwich beams with functionally graded carbon nanotube-reinforced composite face sheets”, *Int. J. Struct. Stab. Dyn.*, **15**(7), 1540011.
- Xu, Y., Ray, G. and Abdel-Magid, B. (2006), “Thermal behavior of single-walled carbon nanotube polymer-matrix composites”, *Compos. Part A: Appl. Sci. Manuf.*, **37**(1), 114-121.
- Yang, J. and Xiang, H. (2007), “Thermo-electro-mechanical characteristics of functionally graded piezoelectric actuators”, *Smart Mater. Struct.*, **16**(3), 784.
- Yang, J., Ke, L.L. and Feng, C. (2015), “Dynamic buckling of thermo-electro-mechanically loaded FG-CNTRC beams”, *Int. J. Struct. Stab. Dyn.*, **15**(8), 1540017.
- Zenkour, A. and Sobhy, M. (2010), “Thermal buckling of various types of FGM sandwich plates”, *Compos. Struct.*, **93**(1), 93-102.

Zhang, C.-L. and Shen, H.-S. (2006), "Temperature-dependent elastic properties of single-walled carbon nanotubes: Prediction from molecular dynamics simulation", *Appl. Phys. Lett.*, **89**(8), 081904.

CC